J Mater Sci (2011) 46:4598–4605
DOI 10.1007/s10853-011-5359-1

Preparation and structural investigation of nanostructured oxide dispersed strengthened steels

Cs. Balázsi · F. Gillemot · M. Horváth · F. Wéber · K. Balázsi · F. Cinar Sahin · Y. Onüralp · Á. Horváth

Received: 26 December 2010 / Accepted: 31 January 2011 / Published online: 10 February 2011

Abstract Although capability of steels has been improved in the past by thermomechanical treatment, utilization of powder metallurgy provides more controlled microstructure, a homogeneous dispersion of nanosized oxide particles in the metal matrix and tailored properties in terms of strength and radiation resistance. This article is summarizing recent results on preparation, structural, and mechanical investigation of oxide dispersed strengthened steel (ODS). Two commercial steel powders, austenitic 17Cr12Ni2.5Mo2.3Si0.1C and martensitic Fe16Cr2Ni0.2C powders have been used as starting materials. Nanosized yttria dispersed martensitic and austenitic sintered steel samples have been realized by powder metallurgical methods. An efficient dispersion of nano-oxides in ODS steels was achieved by employing high efficient attrition milling. A combined wet and dry milling process of fine ceramic and steel particles is proposed. Spark Plasma Sintering (SPS) was applied to realize nanostructured steel compacts. Grains with 100 nm mean size have been observed by SEM in sintered austenitic ODS. In comparison, the sintered martensitic dry milled and martensitic dry and combined milled ODS microstructure consisted of grain size with 100–300 nm in each case. A brittle behavior is shown in all of the cases. The martensitic ODS is two times harder than the austenitic ODS. The bending strength high as 1806.7 MPa was found for the martensitic ODS, whereas 1210.8 MPa was determined for the austenitic ODS. The combined milling assured higher strength and hardness compared to dry milling.

Cs. Balázsi (✉) · F. Wéber
Ceramics and Nanocomposites Department, Research Institute for Technical Physics and Materials Science, Konkoly-Thege M. 29-33, Budapest 1121, Hungary
e-mail: balazsi@mfa.kfki.hu

F. Gillemot · M. Horváth · Á. Horváth
Materials Department, KFKI Atomic Energy Research Institute, Konkoly-Thege M. 29-33, Budapest 1121, Hungary

K. Balázsi
Thin Film Physics Department, Research Institute for Technical Physics and Materials Science, Konkoly-Thege M. 29-33, Budapest 1121, Hungary

F. C. Sahin · Y. Onüralp
Metallurgical and Materials Engineering Department, Istanbul Technical University, Maslak, Istanbul 34469, Turkey

Introduction

Oxide dispersed strengthened steels (ODS) are being developed and investigated for nuclear fission and fusion applications in Japan [1, 2], Europe [3, 4], and the United States [5, 6]. The development of ODS has been conducted in the field of fast reactor fuel cladding application [7–11] and fusion reactor materials application [12]. ODS steels show high strength at high temperatures [13]. As for irradiation effects on the mechanical properties, recent irradiation experiments clearly showed that the ODS steels are highly resistant to irradiation embrittlement (damage as displacement per atom (dpa) of 15) at temperatures between 575 and 775 K [11–13]. ODS steels have attracted attention for advanced nuclear power plants applications such as fast and fusion reactors, because of their superior high-temperature mechanical properties [14, 15]. Although capability of steels has been improved in the past by thermomechanical treatment, utilization of powder metallurgy (PM) provides more controlled microstructure and tailored properties in terms of strength and radiation resistance. For the further improvement of the superior mechanical properties, fundamental understanding of the

influence of composition and heat treatment on the microstructural development is necessary. PM of stainless steel (SS) components constitutes an important and growing segment of the PM industry. The PM processing provides a feasible and economic manufacturing of austenitic SSs components with complex shape and advantages such as good dimensional precision, high surface finish, and good mechanical properties [16–19]. The production of ODS steels involves many processes, such as mechanical alloying, degassing, canning, hot extrusion, and heat treatments. The hot extrusion process among those procedures strongly affects precipitation behavior of oxide particles and their dispersion [20]. Fundamental studies concerning optimization of mechanical milling (MM) processing as well as effects of alloying elements on the high-temperature mechanical strength had been carried out in cooperation with fabrication vendors [21].

This article presents recent results on preparation, structural, and mechanical investigation of ODS steel. Nano-yttria dispersed martensitic and austenitic steel compacts with nanostructure have been realized by powder metallurgical method. An efficient dispersion of nano-oxides in ODS steels was achieved by employing high efficient attrition milling. A combined wet and dry milling process of fine ceramic and steel particles is proposed to achieve efficient oxide dispersion. Spark Plasma Sintering (SPS), a novel sintering method is applied to realize nanostructured steel compacts.

Experimental

The commercial austenitic "Metco 41C" (Fe17Cr12Ni2.5-Mo2.3Si0.1C, AISI Type 316 SS, water atomized, particle size: $-106 + 45$ μm) and martensitic "Metco 42C" (Fe16Cr2Ni0.2C, AISI Type 431 SS, water atomized, $-106 + 45$ μm) powders were used for sample preparation (Table 1). Yttrium oxide with mean particle size 700 nm (grade C) has been purchased from Starck GmbH.

An efficient dispersion of nano-oxides in ODS steels was achieved by employing a high efficient milling process, namely, the attritor milling. In this study, the combined wet (in ethanol) and dry milling process of fine ceramic particles is proposed by the help of mechano-chemical processes assured by attrition milling. The versatile attritor mill can work in wet and dry conditions. In the case of this experiments a high efficient attritor mill (Union Process, type 01-HD/HDDM) equipped with SS setup (tank, agitator, grinding media with 3 mm in diameter) working at 600 rpm for 5 h was employed.

Table 1 Nominal composition of experimental steel powder mixtures (wt%)

Steel powder	Fe	C	Si	Cr	Ni	Mo
Austenitic [22]	Bal.	0.1	1	17	12	2.5
Martensitic	Bal.	0.2	–	16	2	–

For bulk processing, the Field Activated Sintering (FAST) or the SPS method has been used. This technique has a high potential to process „bulk" nanomaterials with good interparticle bonding [23–25]. The external field application is capable to induce fast densification and reasonable control of grain growth during sintering of steels when starting with nanocrystalline powders. The main difference between SPS and hot isostatic pressing (HIP) is the simultaneous application of a pulsed current for SPS, which generates electrical discharges [25, 26]. The electrical discharges do not densify powders; therefore, additional energy is required to increase the final density. This extra energy may be mechanical, as an applied pressure, and thermal by generating higher temperatures than those created by electrical discharge. Sintering of ODS powders was performed by SPS. SPS sintering makes it possible to prepare composites with fully densification at comparatively lower temperature (1210–1220 K in this study) with substantial short holding time (5 min). It also provides a means of precious modification of the kinetics of densification, reactions, and grain growth that are involved in an entire sintering cycle. SPS has been applied with success to a wide range of metals, ceramics (oxides, nitrides, and carbides), and composites [25]. The SPS method is comparable to the conventional hot pressing process, where the precursor powders are loaded in a die and a uni-axial pressure is applied during the sintering. However, instead of using an external heating source, a current, which is typically a few thousands of Ampers (for a few Volts) can pass through the graphite die, the sample, or both. Conduction along the die causes resistance heating, i.e., the die also acts as a heating source. Conduction through the sample may generate a breakdown, arcing, spark, or plasma among powder particles that induce a fast densification process. Using the SPS method, the densification of samples without considerable grain growth process can be achieved within few minutes. A set of composites were sintered by the help of SPS, with the system capacity 10 V and 20,000 A from Sojitz Japan, Dr. Sinter-SPS-7.40MK-VII. The sintering was performed in vacuum, 50 MPa mechanical pressure, temperature 1210–1220 K, and 5 min dwelling time was applied. Circular samples with 50 mm in diameter and 5 mm in thickness have been produced. These samples have been cut by diamond wheels to bars with rectangular geometry ($4 \times 5 \times 30$ mm in dimension). The density of the sintered materials was measured by the Archimedes method. Three point bending strength was determined on Instron

1112 tensile/loading machine equipped with a data acquisition system. The fractured samples obtained after bending tests were passed to electron microscopy investigations. Etching of fracture surfaces of selected samples has been performed by nitric acid aqueous solution. The etched surfaces were investigated by optical microscopy. Microhardness was determined using a Leitz Miniload2 microscope and micro-Vickers hardness tester by applying two loads 5 and 10 N for 10 s. Morphology and microstructure of the powder and the fracture surface of sintered steels were studied by scanning electron microscope (Zeiss-SMT LEO 1540 XB and Jeol JSM-25-SIII). Phase analyses were performed on X-ray diffractometer (Bruker AXS D8) with CuKα radiation.

Results and discussion

The compositions of basic powders were different as given by producer (Table 1). The morphology of the austenitic and martensitic grains is revealed by SEM investigation in Fig. 1. The mean grain size is about 100 μm for each of the starting powders. The austenitic steel powder is comprised of Cr, Ni, Mo, Si, and C next to Fe (Fig. 1a). The martensitic steel powder consists of Fe, Cr, Ni, and C (Fig. 1b).

The combined intensive milling consisted of 5 h wet milling in ethanol at 600 rpm followed by 5 h dry milling (at 600 rpm). Other samples introduced as reference to combined milling and their processing characteristics are presented in Table 2.

The structure of powders is considerably changed after these intensive milling as shown in Fig. 2. The metal grain size of austenitic ODS powder is around 2 μm in average; however, these grains are stacked to 5 and 20 μm aggregates (Fig. 2a). Globular and lamellar shaped grains may be also observed. The martensitic ODS powder grain size is also considerably lowered compared to the initial grain size of the starting powder (Fig. 2b). The average grain size is 1–2 microns, but the same sticking tendency is revealed as in the case of austenitic ODS powder. Because of this the

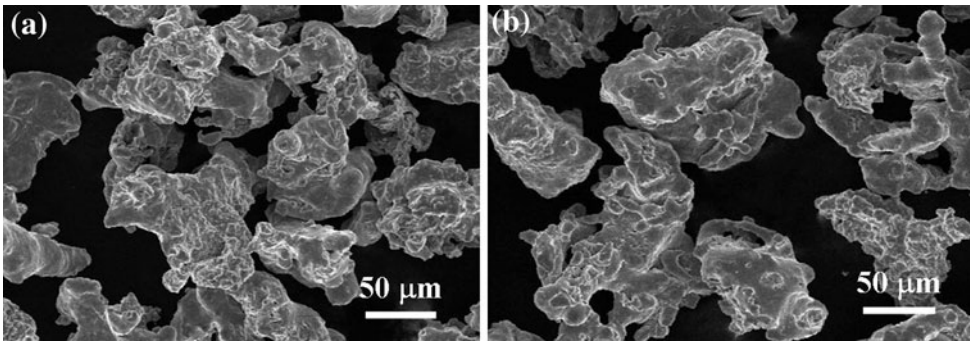

Fig. 1 SEM images of commercial steel powders. **a** Austenitic; **b** martensitic

Table 2 The milling parameters of the steel samples

Sample	Steel powder	Milling
A1	Austenitic + 1 wt% Y_2O_3	Combined (wet and dry) at 600 rpm for 5 h each
A2	Austenitic	Dry (600 rpm for 5 h)
M1	Martensitic + 1 wt% Y_2O_3	Combined (wet and dry) at 600 rpm for 5 h each
M2	Martensitic + 1 wt% Y_2O_3	Dry (600 rpm for 5 h)
M3	Martensitic	Dry (600 rpm for 5 h)

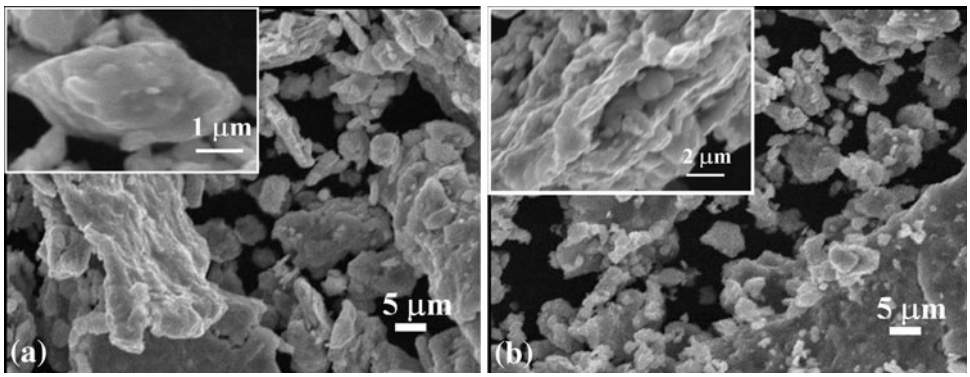

Fig. 2 SEM images of ODS steel powders prepared by combined milling (5 h wet milling in ethanol followed by 5 h dry milling). **a** Austenitic ODS powder with 1 wt% Y_2O_3 addition, higher magnification in *inset* (sample A1); **b** martensitic ODS powder with 1 wt% Y_2O_3 addition, higher magnification in *inset* (sample M1)

mean secondary aggregates size can reach 5–10 microns, as it is shown in Fig. 2.

Striking differences between combined milled samples (Fig. 2) and dry milled powder samples may be observed on Fig. 3. SEM images of reference steel powders prepared by 5 h dry milling of austenitic powder (sample A2), martensitic ODS powder with 1 wt% Y_2O_3 addition (sample M2), and martensitic powder (sample M3) show that their structure is more compact after milling. Although the grain size is similar to powders gained by combined milling (1–2 microns), the secondary aggregates preserved the morphology and size of 80–100 microns of starting powders. It can be concluded that the disintegration is achieved only partially by dry milling. In the same time, the combined milling assures a more efficient grain size reduction.

The elemental mapping of austenitic and martensitic ODS powders containing 1 wt% yttrium oxide as dispersed oxides made with the help of energy dispersive spectroscopy are presented in Fig. 4.

It is easy to observe that besides the iron, nickel and chrome are the main components of the steel powders. A non-homogeneous distribution of carbon and molybdenum is revealed (red and orange areas). The carbon is originated from starting powder (0.1 wt%), but a lower amount might be introduced by intensive milling as well. The most interesting, however, is the distribution of yttrium (introduced in form of yttrium oxide) after intensive milling shown in Fig. 4b and d. Addition of 1 wt% yttrium oxide to the starting powder has the aim to achieve improvements in mechanical properties at high temperature (higher than 775 K). The EDS mapping showed that the steel grains are covered homogeneously by yttrium oxide nanoparticles (Fig. 4b).

The sintering parameters of the steel samples are presented in Table 3.

Fracture surfaces of ODS samples (obtained after bending test) prepared by SPS are presented in Fig. 5. The densification of samples without considerable grain growth is achieved within few minutes (Table 3). The fast densification process using the SPS method assures the preservation of the starting morphology of steel powders resulted from intensive milling. SEM micrograph with high magnification shows steel grains with 100 nm mean size in austenitic ODS. In comparison, the martensitic ODS microstructure consists of steel grains with 100–300 nm in size.

In contrast to high magnification SEM micrographs presented above, the etched micrographs show the overall microstructure as resulted from milling and consecutive sintering process of different steel samples (low magnification optical micrographs in Fig. 6. Fracture surface of sintered austenitic (Fig. 6a and c) and martensitic steels

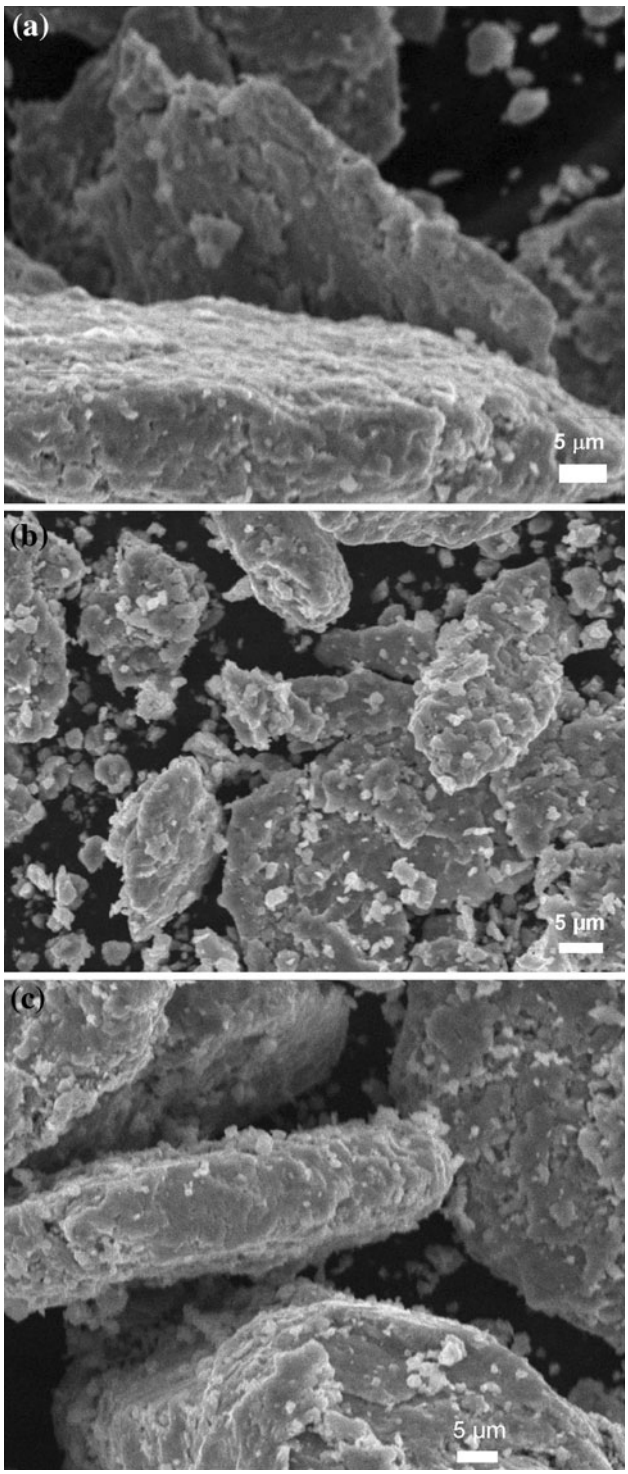

Fig. 3 SEM images of reference steel powders prepared by 5 h dry milling. **a** Austenitic powder (sample A2); **b** martensitic ODS powder with 1 wt% Y_2O_3 addition (sample M2); **c** martensitic powder (sample M3)

(Fig. 6b and d) processed by combined (Fig. 6a and b) or dry milling (Fig. 6c and d) can be seen in Fig. 6. It can be concluded that the combined (wet and dry) milling with consecutive SPS sintering is more efficient in the case of

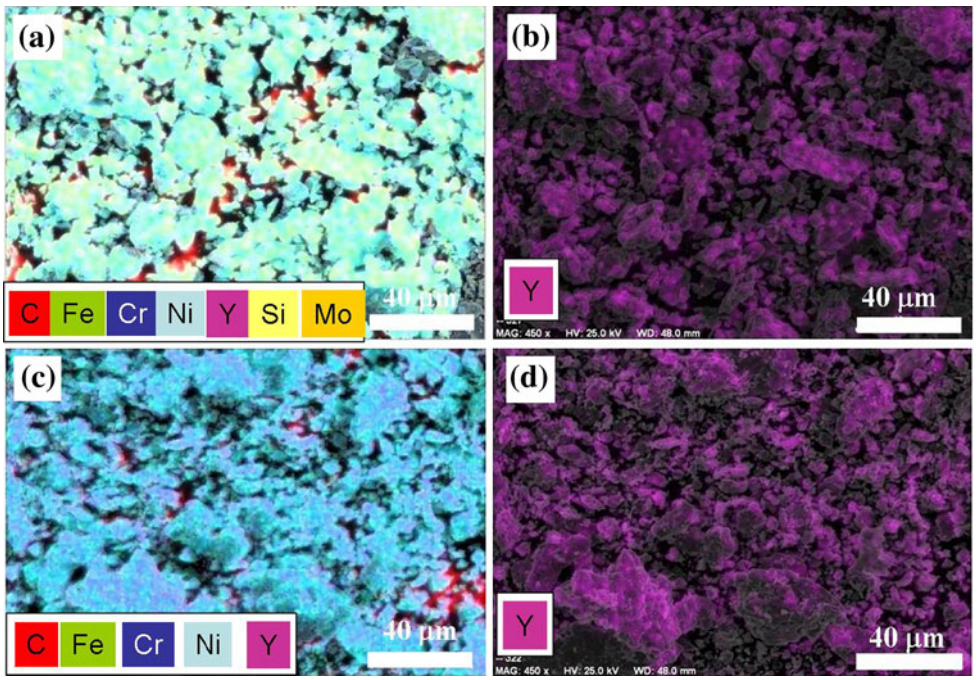

Fig. 4 Elemental analysis of austenitic ODS powder prepared by combined milling. **a** EDS map of different phases (C—*red*, Fe—*green*, Cr—*dark blue*, Ni—*blue*, Y—*purple*, Si—*yellow*, Mo—*orange*); **b** EDS map of yttrium. Elemental analysis of martensitic ODS powder prepared by combined milling; **c** EDS map of different phases (C—*red*, Fe—*green*, Cr—*dark blue*, Ni—*blue*, Y—*purple*); **d** EDS map of yttrium (Color figure online)

Table 3 Sintering parameters of the steel samples

Sample	Steel powder	Sintering parameters			Relative density (%)
		Temperature (°C)	Pressure (MPa)	Holding time (min)	
A1	Austenitic + 1 wt% Y_2O_3	945	50	5	90
A2	Austenitic	930	50	5	94.7
M1	Martensitic + 1 wt% Y_2O_3	937	50	5	92.1
M2	Martensitic + 1 wt% Y_2O_3	930	50	5	92.1
M3	Martensitic	920	50	5	94.1

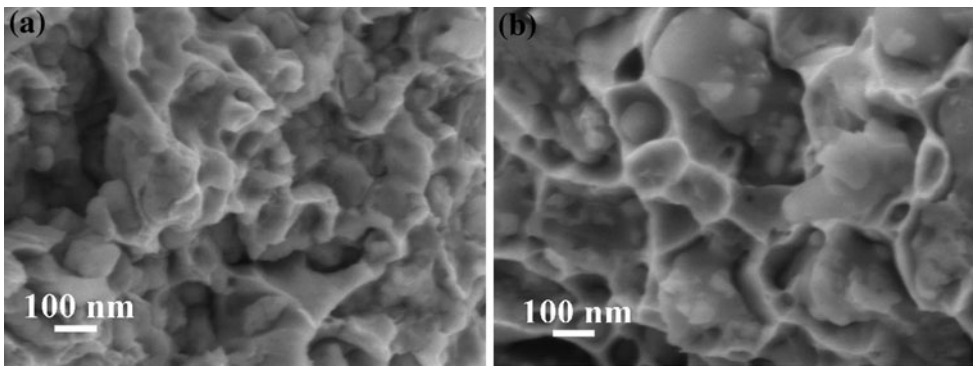

Fig. 5 SEM images of fracture surface of sintered ODS processed by combined milling showing dense nanostructure. **a** austenitic ODS with 1 wt% Y_2O_3 addition (sample A1); **b** Martensitic ODS with 1 wt% Y_2O_3 addition (sample M1)

austenitic sample (Fig. 6a). The submicron grains resulted from intensive milling are presented by black areas of micrographs. There can be lamellar grains 50 micron in length that resulted from severe plastic deformation of starting grains. If we compare the morphology and black areas in the Fig. 6a and b, then we may conclude that the milling was less efficient in the case of martensitic ODS. Submicron grains have been appeared (black grains), but huge percentage of the microstructure consists of 100 micron grains in length (white areas).

The dry milled samples, both austenitic or martensitic, present huge white grains with 200 micron in length (Fig. 6c and d). Dry milling compared to combined milling resulted lower efficiency, non-disintegrated grains are

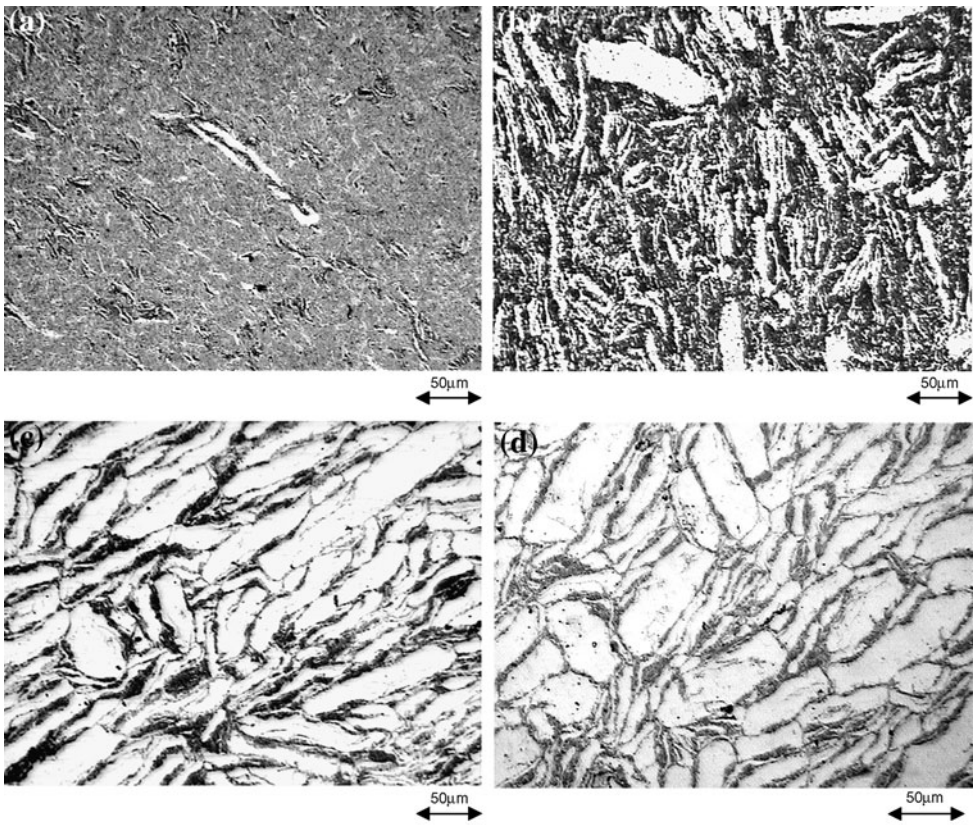

Fig. 6 Etched micrographs of fracture surface of sintered steel powders processed by combined or dry milling. **a** Austenitic ODS with 1 wt% Y_2O_3 addition (combined milling, sample A1); **b** martensitic with 1 wt% Y_2O_3 addition (combined milling, sample M1); **c** austenitic (dry milling, sample A2); and **d** martensitic (dry milling, sample M3)

present in steel structure. The partly disintegrated submicron size particles have been found to be agglomerated in intergranular places (as shown in Figs. 5 and 6).

Phase analyses performed by X-ray measurements are shown in Fig. 7. In the case of commercial austenitic steel powder, the main lines of austenite cubic Cr0.19Fe 0.7Ni0.11 phase (JCPDFWIN 33-0397) and cubic FeNi (JCPDFWIN 03-1209) have been assigned. In the case of commercial martensitic powder, the main lines of martensite cubic Cr0.19Fe0.7Ni0.11 phase (JCPDFWIN 33-0397) and cubic FeCr (JCPDFWIN 34-0396) can be observed.

In the case of commercial austenitic powder where the grain mean size was 100 microns the CrFeNi phase is dominant ($2\theta = 43.55°$, 50.75°, and 74.6°). However, the FeNi phase is also present in the powder structure. This is demonstrated by EDS measurements, but the cubic FeNi phase main lines are present on XRD ($2\theta = 44.5°$, 64.2°, and 82.1°). The XRD analyses are showing the microstructural changes of powder during milling and the after sintering steps (Fig. 7a). The dominant CrFeNi phase in commercial powder can hardly be observed after milling, but the FeNi main lines became stronger.

This may be related to intensive milling that resulted in fragmented grains. The broadening of peaks is also supported by the SEM observations showing the decreased steel grain sizes. No other phase is evolved during the sintering, but the grain size is further decreased, as it was shown by SEM. In the commercial martensitic powder, the cubic FeCr phase ($2\theta = 44.7°$, 65.4°, and 82.3°) is dominant, but CrFeNi is also present (Fig. 7b).

In austenitic powder 12 wt% Ni is present, whereas only 2 wt% Ni can be found in composition of martensitic powder. The grain size is decreasing and no new phases are developing during milling similar to austenitic powder. FeCr is characterizing the structure after sintering. The broadening of the peaks may be related to decrease of grain size during sintering. This is consistent with SEM observations. The location, dispersion, and evolution of yttria in steel matrix is of particular interest in ODS research [27]. In this study, however, the main lines of Y_2O_3 (JCPDFWIN 82-2415) expected at $2\theta = 29.15°$, 33.79°, 48.53°, and 57.62° could not be observed on the XRD spectra.

Three point bending strength was determined on Instron 1112 tensile/loading machine equipped with a data acquisition system [19]. Sintered ODS steel rectangular bars, $4 \times 5 \times 30$ mm in dimension, have been used for testing. The bending strength–strain curves related to sintered austenitic and martensitic ODS processed by combined or dry milling are presented in Fig. 8.

A brittle behavior is shown in each case. A bending strength about 1806.7 MPa was found for the martensitic

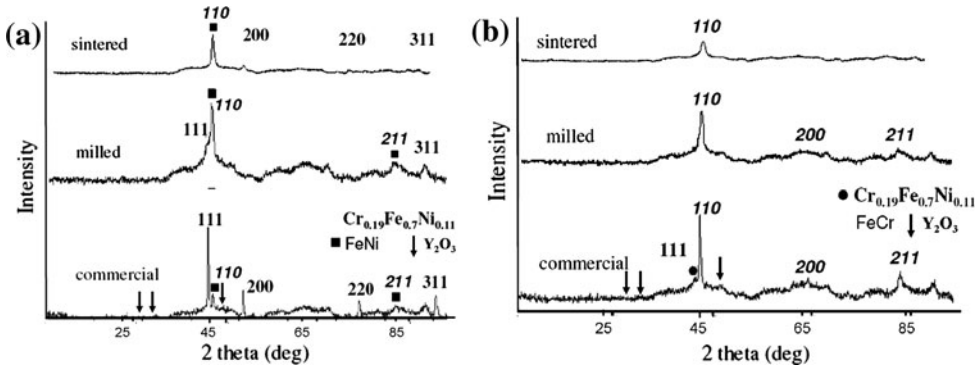

Fig. 7 XRD spectra of as received combined milled (wet and dry) powder and sintered samples. **a** Austenitic (sample A1); **b** martensitic (sample M1)

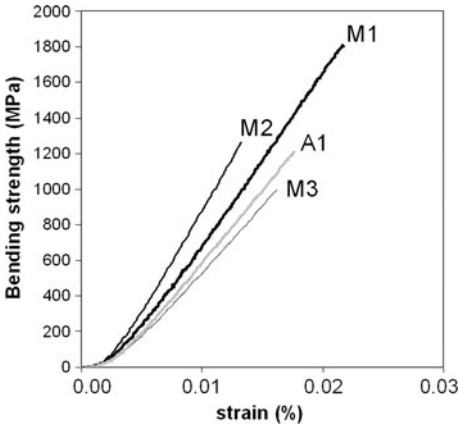

Fig. 8 Strength–strain curves of sintered austenite and martensite ODS samples processed by combined or dry milling (sample A2 not measured—n.m.)

ODS, whereas 1210.8 MPa was determined for the austenitic ODS.

The addition of ittria resulted in an increase of bending strength. The dry milled sample (M1) has 1000.7 MPa, whereas the dry milled ODS sample (M2) has 1261.2 MPa. By applying combined milling, however, the bending strentgh could increase even higher. Bending strength high as 1806.7 MPa for sample (M3) was achieved.

The microhardness of sintered ODS steel was measured at loads of 5 and 10 N for 10 s, whereas elastic modulus was calculated from strength–strain curves (Table 4). As resulted from microhardness measurements, the martensitic ODS is twice as hard as the austenitic ODS. The combined milling has a beneficial role to hardness increase in both austenitic and martensitic steels.

Table 4 Hardness and calculated elastic modulus of austenite and martensite ODS steels processed by combined or dry milling, measured at loads of 5 and 10 N

Sample	HV (GPa) (5 N)	HV (GPa) (10 N)	*E* (GPa)
Austenitic ODS (A1)	4.07 ± 0.18	5.31 ± 0.48	81
Austenitic (A2)	2.92 ± 0.22	3.68 ± 0.27	n.m.
Martensitic ODS (M1)	7.23 ± 0.29	8.03 ± 0.43	96
Martensitic ODS (M2)	5.49 ± 0.3	5.53 ± 0.28	112.8
Martensitic (M3)	6.09 ± 0.25	7.42 ± 0.3	72.3

Summary

This article summarizes recent results on ODS steels produced by intensive milling together with SPS. The structure of powders is considerably changed after intensive combined (wet and dry) milling. The grain size of steel powders has been reduced from 50 to 100 μm to 1–2 microns in average after milling; however, these grains were stacked to 5–20 microns aggregates presenting a non-regular morphology in the same time. It can be concluded that the disintegration of starting grains is achieved only partially by dry milling. Although the grain size is similar to powders obtained by combined milling (1–2 microns), the secondary aggregates preserved the morphology and size of 80–100 microns of starting powders. In contrast, the combined milling assures a more efficient grain size reduction. Dense samples showing nanostructural characteristics have been achieved after sintering at only 1210–1220 K for 5 min by SPS. Grains of steel with 100 nm mean size have been observed by SEM at high magnifications in austenitic ODS. In comparison, the martensitic ODS microstructure consisted of grain size with 100–300 nm. A brittle behavior is shown in each case. The martensitic ODS is twice as hard as the austenitic ODS. The combined milling resulted in hardness and bending strength increase. Further studies are needed to demonstrate the dual beneficial role of developing nanostructure and oxide nano-dispersions in steel to the mechanical properties at ambient and elevated temperatures.

Acknowledgements This study was supported by EFDA, FEMAS and TAMOP 4.2.2. - 08/1-2008-0016. Thanks for XRD and SEM measurements to Dr. Z.E. Horváth, Dr. A.L. Tóth and L. Illés.

References

1. Ukai S, Nishida T, Okada H, Okuda T, Fujiwara M, Asabe K (1997) J Nucl Sci Technol 34:256
2. Ukai S, Yoshitake T, Mizuta S, Matsudaira Y, Hagi S, Kobayashi T (1999) J Nucl Sci Technol 36:710
3. Alamo A, Decours J, Pigoury M, Foucher C (1990) Structural applications of mechanical alloying. ASM International, Materials Park
4. Alamo A, Regle H, Pons G, Bechade LL (1992) Mater Sci Forum 88–90:183
5. Mukhopadhyay DK, Froes FH, Gelles DS (1998) J Nucl Mater 258–263:1209
6. Miller MK, Kenik EA, Russell KF, Heatherly L, Hoelzer DT, Maziasz PJ (2003) Mater Sci Eng A 353:140
7. Ukai S, Harada M, Okada H, Inoue M, Nomura S, Shikakura S, Asabe K, Nishida T, Fujiwara M (1993) J Nucl Mater 204:65
8. Ukai S, Harada M, Okada H, Inoue M, Nomura S, Shikakura S, Nishida T, Fujiwara M, Asabe K (1993) J Nucl Mater 204:74
9. Fischer JL (1978) US Patent 4,075,010, 21 Feb 1978
10. Yun T, Guangzu L, Bingquan S (2000) 6th Japan–China symposium on materials for advance energy systems and fission and fusion engineering, RIAM, Kyushu University, 4–6 Dec 2000
11. Kimura A, Sawai T, Shiba K, Hishinuma A, Jitsukawa S, Ukai S, Kohyama A (2003) Nucl Fusion 43:1246
12. Kimura A, Cho HS, Lee JS, Kasada R, Ukai S, Fujiwara M (2004) In: Proceedings of the 2004 international congress on advances in nuclear power plants, p 2070
13. Kimura A (2005) Mater Trans 46:394
14. Huet JJ (1967) Powder Metall 10:208
15. Huet JJ, Leroy V (1974) Nucl Technol 24:216
16. Borgioli F, Galvanetto E, Bacci T et al (2002) Surf Coat Technol 149:192
17. Sandberg O, Jönson L (2003) Adv Mater Process 12:37
18. Lindskog P (2004) Powder Metall 47:6
19. Koszor O, Horváth A, Weber F, Balázsi K, Gillemot F, Horvath M, Fényi B, Balázsi C (2009) Key Eng Mater 409:237
20. Sakasegawa H et al (2008) J Alloys Compd 452:2
21. Okuda T, Nomura S et al. (1989) Proceedings on Symposium. Sponsored by the TMS Powder Metallurgy Committee, Indiana, p 195
22. Syed AA, Denoirjean A, Denoirjean P, Labbe JC, Fauchais P (2004) In: Thermal Spray 2004, Advances in Technology and Application, Proceedings of the international thermal spray conference, Osaka, Japan, pp 100–105, 10–12 May 2004
23. Palm M, Preuhs J, Sauthoff G, Mater J (2003) Process Technol 136:114
24. Groza JR, Ribaud SH, Yamazaki K (1992) J Mater Res 7:2643
25. Groza JR, Curtis JD, Kramer M (2000) J Am Ceram Soc 83:1281
26. Gang JL, Grosdidier T, Bozzolo N, Launois S (2007) Intermetallics 15(2):108
27. Zhang L, Ukai S, Hoshino T, Hayashi S, Qu X (2009) Acta Mater 57/12:3671